Figure S1

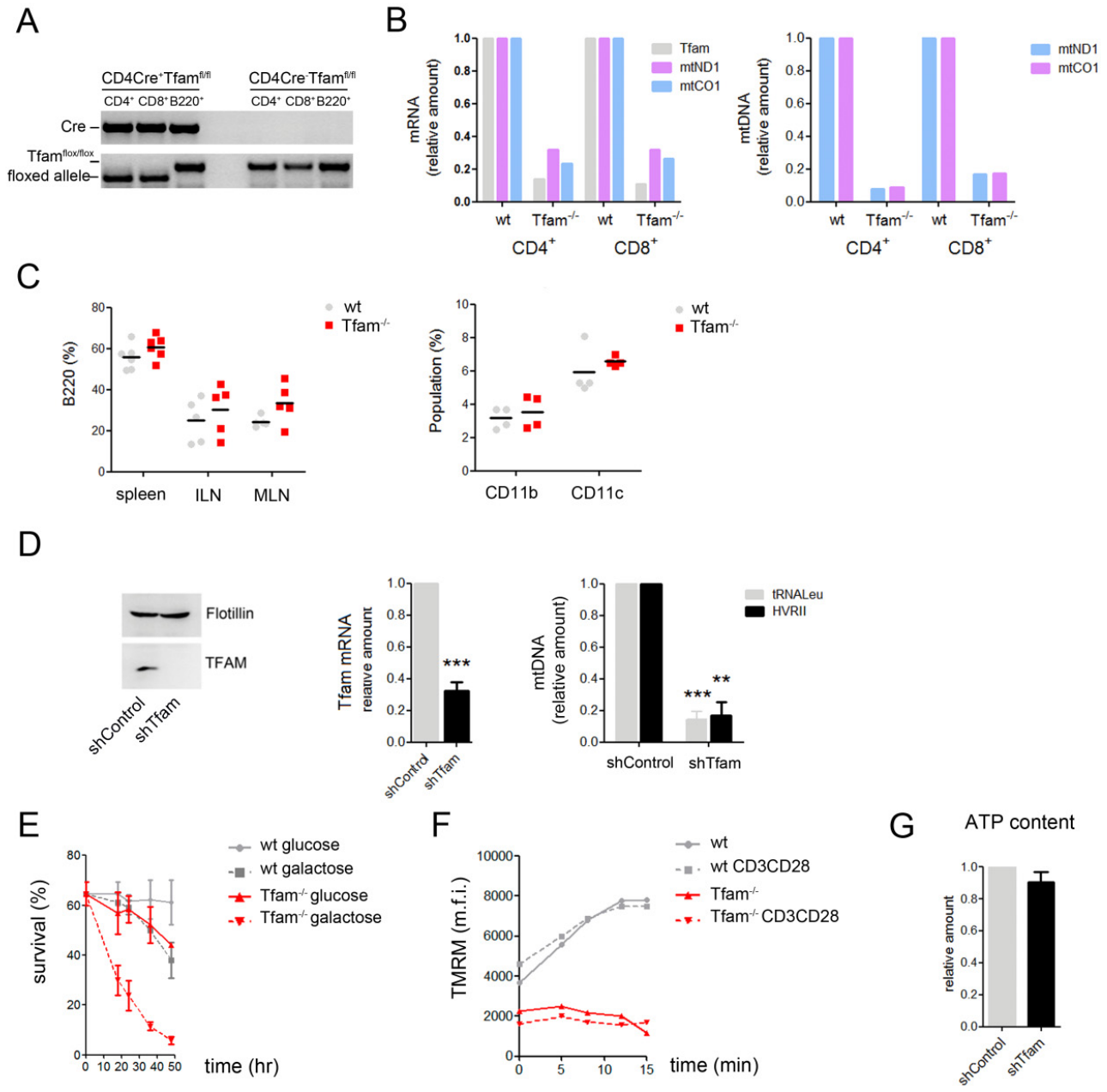
A
CD4Cre+Tfamfl/fl
CD4+ CD8+B220+
CD4Cre-Tfamfl/fl
CD4+ CD8+B220+
Cre
Tfamflox/flox
floxed allele
B
mRNA (relative amount)
Tfam
mtND1
mtCO1
wt
Tfam-/-
CD4+
CD8+
mtDNA (relative amount)
C
B220 (%)
spleen
ILN
MLN
Population (%)
CD11b
CD11c
D
Flotillin
TFAM
shControl
shTfam
Tfam mRNA relative amount
mtDNA (relative amount)
tRNALeu
HVRII
E
survival (%)
wt glucose
wt galactose
Tfam-/- glucose
Tfam-/- galactose
time (hr)
F
TMRM (m.f.i.)
wt
wt CD3CD28
Tfam-/-
Tfam-/- CD3CD28
time (min)
G
ATP content
relative amount

Figure S2

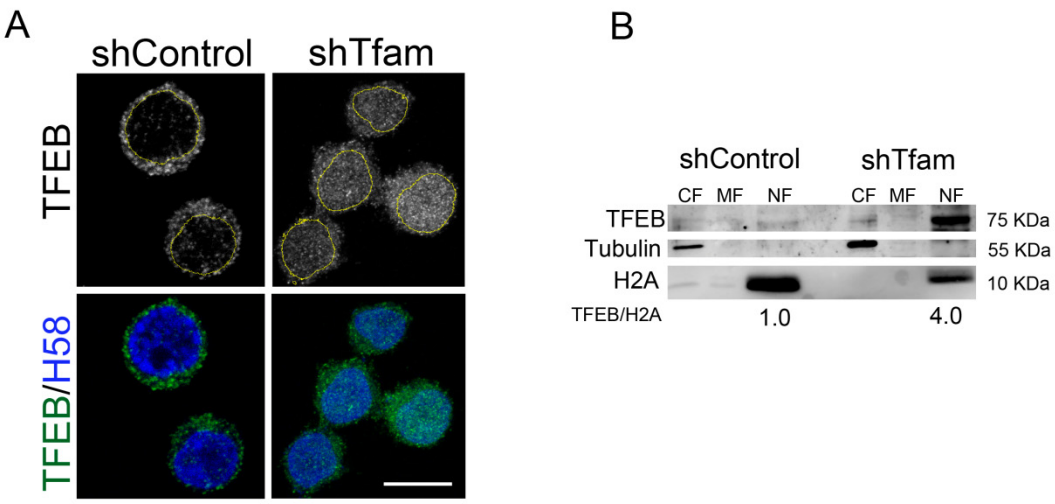
A
shControl
shTfam
TFEB
TFEB/H58
B
shControl
shTfam
CF MF NF CF MF NF
TFEB
Tubulin
H2A
75 KDa
55 KDa
10 KDa
TFEB/H2A
1.0
4.0

Figure S3

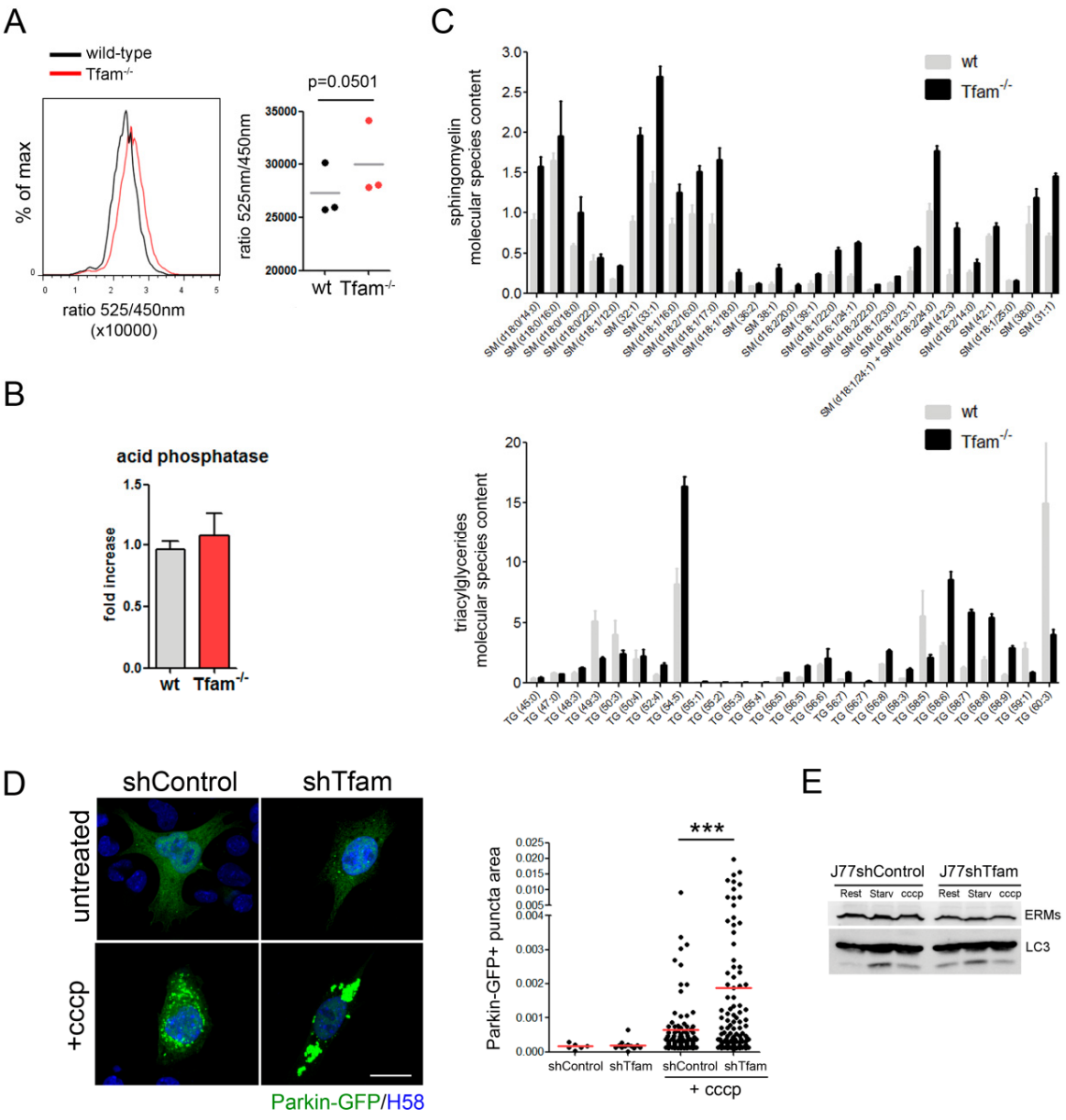
A
wild-type
Tfam-/-
% of max
ratio 525/450nm
(x10000)
p=0.0501
ratio 525nm/450nm
wt
Tfam-/-
B
acid phosphatase
fold increase
wt
Tfam-/-
C
wt
Tfam-/-
sphingomyelin
molecular species content
triacylglycerides
molecular species content
D
shControl
shTfam
untreated
+cccp
Parkin-GFP/H58
Parkin-GFP+ puncta area
***
shControl
shTfam
shControl
shTfam
+ cccp
E
J77shControl
J77shTfam
Rest
Starv
cccp
Rest
Starv
cccp
ERMs
LC3

Figure S4

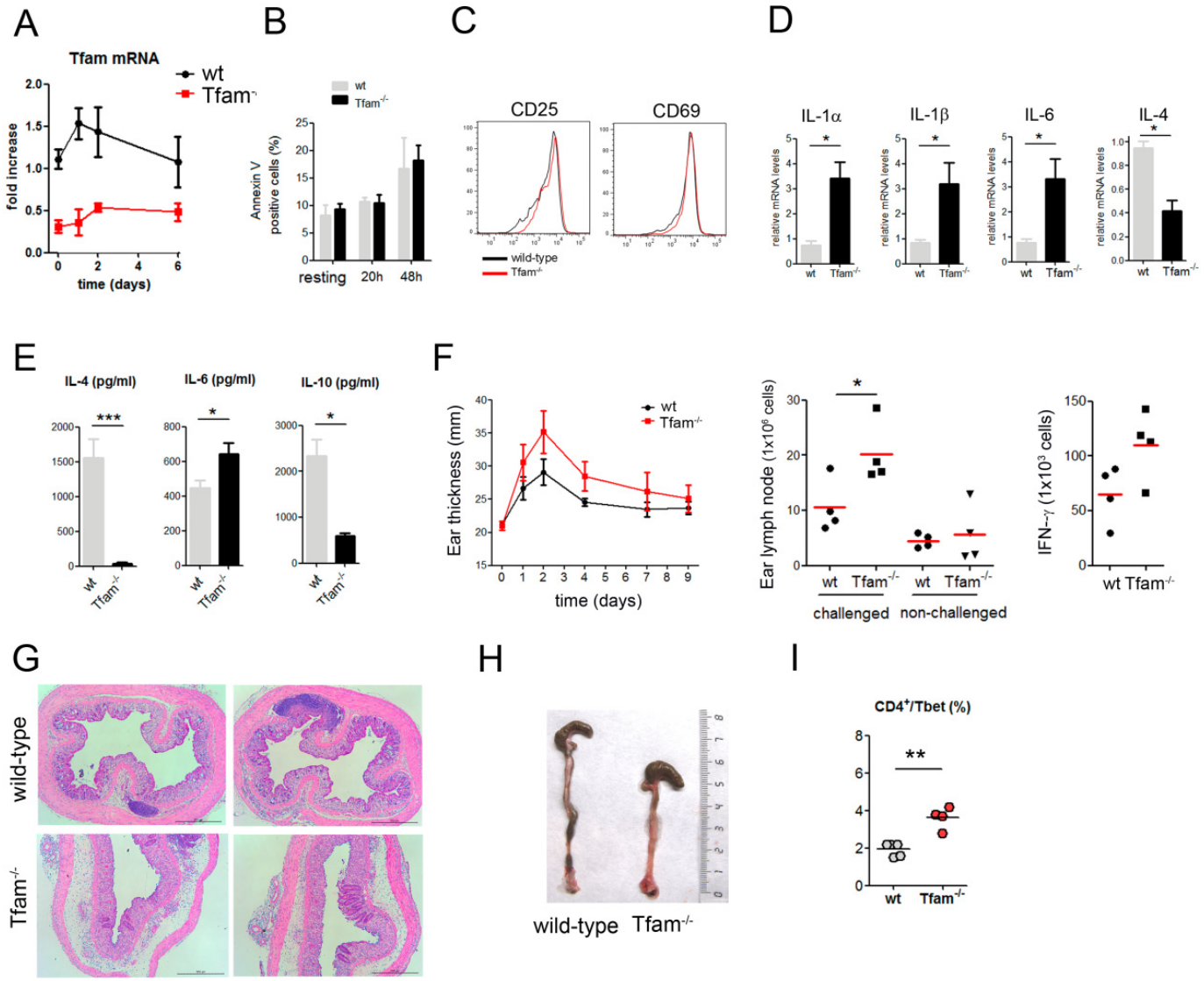
A
Tfam mRNA
wt
Tfam-/-
fold increase
time (days)
B
wt
Tfam-/-
Annexin V positive cells (%)
resting
20h
48h
C
CD25
CD69
wild-type
Tfam-/-
D
IL-1α
IL-1β
IL-6
IL-4
relative mRNA levels
E
IL-4 (pg/ml)
IL-6 (pg/ml)
IL-10 (pg/ml)
F
Ear thickness (mm)
time (days)
Ear lymph node (1x10^6 cells)
challenged
non-challenged
IFN-γ (1x10^3 cells)
G
wild-type
Tfam-/-
H
wild-type
Tfam-/-
I
CD4+/Tbet (%)

Figure S5

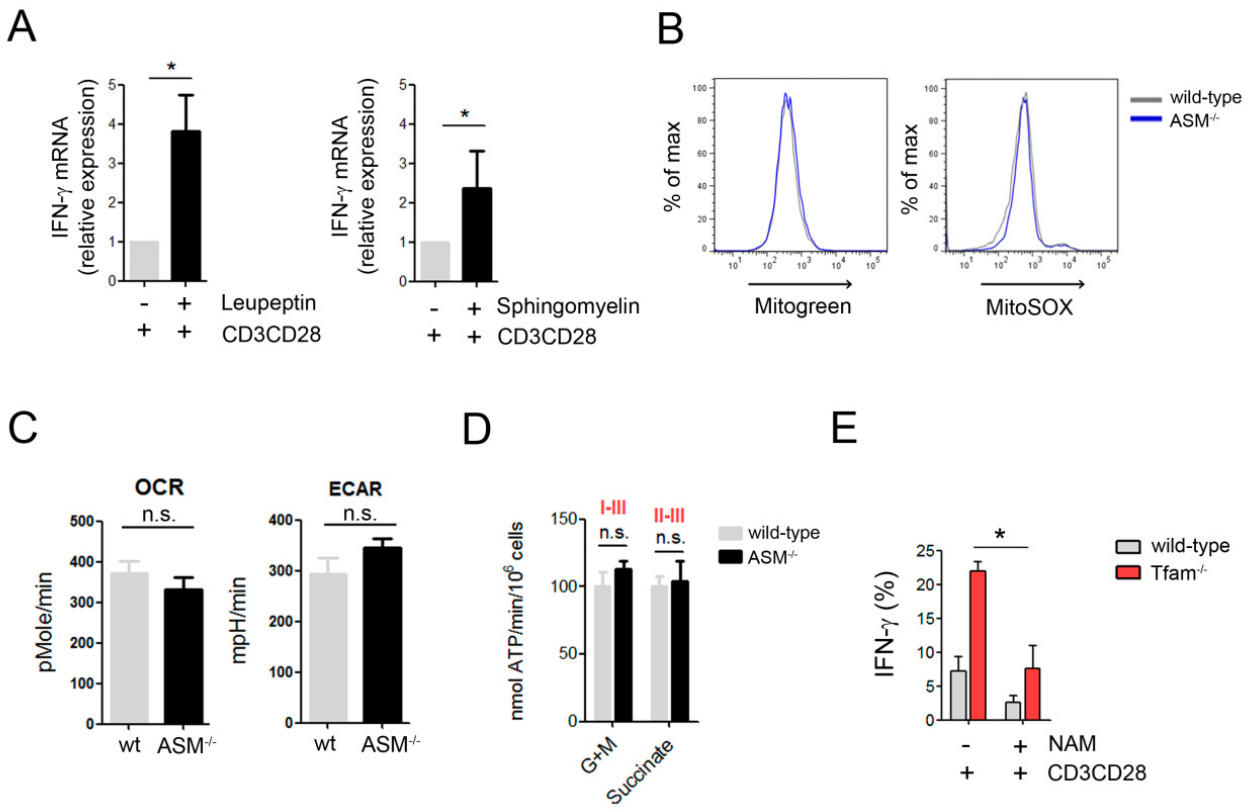
A
IFN-γ mRNA (relative expression)
*
- + Leupeptin
+ + CD3CD28
IFN-γ mRNA (relative expression)
*
- + Sphingomyelin
+ + CD3CD28
B
% of max
Mitogreen
% of max
MitoSOX
wild-type
ASM-/-
C
OCR
n.s.
pMole/min
wt
ASM-/-
ECAR
n.s.
mpH/min
wt
ASM-/-
D
I-III
II-III
n.s.
n.s.
nmol ATP/min/10^6 cells
G+M
Succinate
wild-type
ASM-/-
E
*
IFN-γ (%)
- + NAM
+ + CD3CD28
wild-type
Tfam-/-

Supplemental Figure Legends

Supplemental Figure 1. (A) Naive $CD4^+$, $CD8^+$ and $B220^+$ cells were isolated by magnetic separation from $CD4Cre^+$ *Tfam*$^{fl/fl}$ (*Tfam*$^{-/-}$) and $CD4Cre^-$ *Tfam*$^{fl/fl}$ (wild-type) 4-week-old mice. DNA was isolated and gel shows PCR products from Cre and Tfam alleles. (B) Naive $CD4^+$ and $CD8^+$ T cells from spleen and lymph nodes of 4-week-old mice. Left panel: RT-PCR determination of the mRNA levels of Tfam and the mitochondrial DNA-encoded subunits mtND1 and mtCO1, expressed relative to wild-type cells. Right panel: levels of mtDNA relative to genomic DNA (gDNA) assessed by PCR in naive $CD4^+$ and $CD8^+$ T cells. (C) Left panel: percentage of B cells (B220+) in the spleen, inguinal lymph nodes (ILN) and mesenteric lymph nodes (MLN). Right panel: percentage of myeloid cells (CD11b) and dendritic cells (CD11c) in the spleen ($n \leq 4$). (D) Jurkat T cells were stably transfected with shControl and shTfam RNAs. Left: western blot detection of Tfam protein. Flotillin was used as loading control. Center: Relative Tfam mRNA expression by RT-PCR. Right: mtDNA content relative to gDNA by PCR. (E) T lymphoblast were grown in presence of either glucose or galactose, and the percentage of viable cells was assessed by HOECHST58 exclusion by flow cytometry at the indicated times. Data are means ± SEM of two independent experiments. (F) Resting or CD3/CD28-activated T cells were labeled with TMRM and mitochondrial membrane potential was assessed by flow cytometry upon oligomycin addition at the indicated times. (G) Cellular ATP content in shTfam Jurkat T cells relative to the ATP levels in shControl cells (n=3). Data are means ± SEM; *p<0.05, **p<0.01, ***p<0.001, Student's t-test.

Supplemental Figure 2. (A) Confocal analysis of TFEB (green) in Jurkat T cells stably transfected with shControl and shTfam RNAs. Nuclei were stained with HOECHST58 (blue). Scale bar represents 10 μm. (B) Western blot analysis of TFEB in subcellular fractions of shControl or shTfam Oli-Neu cells. Cytosol, membranous organelles and nuclear fractions were blotted for TFEB, tubulin (cytoplasmic marker), and histone 2A (H2A) (nuclear marker). Densitometric analyses were performed, and numbers represent the ratio of nuclear TFEB to H2A. CF, cytoplasmic fraction; MF, membrane fraction; NF, nuclear fraction.

Supplemental Figure 3. (A) Analysis of lysosomal pH in T-lymphoblasts with the pH-sensitive probe LysoSENSOR DND160. LysoSensor DND160 undergoes a pH-dependent emission shift to longer wavelengths in acidic environments. The ratio between the 525nm and 450 nm emission is shown from three independent experiments (paired t-test, p= 0.0501). (B) Acid phosphatase activity in wt and *Tfam*$^{-/-}$ T lymphoblasts. (C) Cell lipidomic signatures of wild-type and *Tfam*$^{-/-}$ cells obtained from three mice per genotype by ultra performance liquid chromatography coupled to mass spectrometry (UPLC-MS). Sphingomyelin and triacylglycerides metabolites extracted from wild-type and *Tfam*$^{-/-}$ T lymphoblasts, ordered from left to the right according to carbon number and degree of saturation of acyl chains. (D) Mitophagy analysis by confocal microscopy in shControl and shTfam Oli-Neu cells transfected with Parkin-GFP and left untreated or cccp-treated during 4 hr. Images show maximal projections of confocal images, parkin-GFP (green), HOECHST58 (blue). Scale bar represents 10 μm. Graph show quantification from the area of at least 100 vesicles in two independent experiments. (E) Western blot analysis of LC3 in J77 shControl and shTfam cells in resting, starving and CCCP treatments.

Supplemental Figure 4. (A) Tfam mRNA levels by RT-PCR in wild-type and *Tfam*$^{-/-}$ CD4^{+} T cells during T cell activation with CD3/CD28 during the indicated times. (B) Flow cytometry analysis of Annexin V staining in resting and activated cells for the indicated times. Data are means ± SEM of three independent experiments. (C) Flow cytometry analysis of CD69 and CD25 expression in activated wild-type and *Tfam*$^{-/-}$ CD4^{+} T cells. (D) RT-PCR detection of the mRNA levels of IL-1α, IL-1β, IL-6 and IL-4 in wild-type and *Tfam*$^{-/-}$ CD4^{+} T cells activated for 6 days with anti-CD3/CD28. Results are expressed as the relative mRNA levels with respect to wild-type cells. Data are means ± SEM (n=3, *p<0.05, Student's t-test). (E) CD4^{+} T cells activated with anti-CD3/CD28 (6 days). IL-4, IL-6, IL-10 cytokine levels in the supernatant measured by ELISA. Data are means ± SEM (n=5, *p<0.05, ***p<0.001, Student's t-test). (F) Wild-type and *Tfam*$^{-/-}$ mice were sensitized with 3.0 % oxazolone on the abdomen. After 4 days, (day 0 on the graph), the ears of the mice were challenged with 1.0 % oxazolone and swelling was monitored by measuring ear thickness on the indicated days, left panel. Data are means ± SEM of 5 wild-

type and 5 *Tfam*$^{-/-}$ mice. Center panel shows the number of cells in the lymph nodes from challenged and non-challenged ears. Right panel shows IFN-γ producing CD4^{+} T cells in the challenged ear lymph nodes from wt and *Tfam*$^{-/-}$ mice. Data are means of 4 wild-type and 4 *Tfam*$^{-/-}$ mice. (G) H&E staining of colon sections in wild-type and *Tfam*$^{-/-}$ mice on day 7 after DSS treatment. (H) Representative image shows the colon length in wild-type and *Tfam*$^{-/-}$ mice on day 7 after DSS treatment. (I) T-bet-producing CD4^{+} T cells in the mesenteric lymph nodes from wild-type and *Tfam*$^{-/-}$ mice. Data are means ± SEM of two independent experiments; *p<0.05, **p<0.01, Student's t-test.

Supplemental Figure 5. (A) Quantitative mRNA levels of inflammatory cytokines in CD4^{+} T cells activated with anti-CD3/CD28 (6 days) in the presence of leupeptin (1 μM) or sphingomyelin (25 μM). Results are expressed as the mRNA levels relative to untreated cells, and data are means ± SEM, n=3, *p<0.05, Student's t-test. (B) Flow cytometry analysis of mitochondrial mass (Mitogreen) and mROS (MitoSOX) in T lymphoblasts. (C) The oxygen consumption rate (OCR) and extracellular acidification rate (ECAR) were measured in real time in CD4^{+} T cells in the presence of glucose. Panels show the basal OCR and ECAR from two independent experiments. (D) Glutamate- and pyruvate-driven ATP-dependent production in wt and ASM$^{-/-}$ T lymphoblasts. (E) Naive CD4^{+} T cells from *Tfam*$^{-/-}$ and wild-type mice were activated with anti-CD3/CD28 in the presence or absence of NAM. After 3 days, T cells were incubated with PMA/ionomycin and brefeldin followed by intracellular flow cytometry analysis of IFN-γ. Graphs show quantification of IFN-γ-producing cells in 3 independent experiments. *p<0.05 Student's t-test).

Supplemental Experimental procedures

Antibodies and reagents

Antibodies for western blot and immunofluorescence were as follows: anti-tubulin, anti-flotillin and anti-p62 from Sigma-Aldrich; anti-CD63 and anti-TOM20 from Santa Cruz Biotechnology; anti-TFAM, anti-HRS, anti-COX1, anti-NDUFA9, anti-Core-1, anti-SDHA (FpSDH) and anti-TSG101 from Abcam; anti-TFEB from Bethyl Laboratories and from Cell Signaling; anti-LAMP1 from Biolegend; anti-LBPA from Tebu-Bio; anti-LC3, anti-p-AMPK (Thr172), anti-AMPK, and anti-HisH4 from Cell Signaling; and anti-MnSOD from Enzo Life Sciences. Anti-ERMs were produced in our laboratory. Goat anti-mouse peroxidase and goat anti-rabbit peroxidase were from Thermo Scientific. Poly-L-lysine (PLL), Concanavalin A (ConA), phorbol myristate acetate (PMA), ionomycin and Nicotinamide (NAM) were from Sigma. Phalloidin647, tubulin-FITC, Alexa 488-, 647-, and 568-labeled secondary antibodies, Cell Violet, Indo-1, tetramethylrhodamine methyl ester (TMRM), HOECHST58, Mitotracker green, MitoSOX and Lysotracker were from Life Technologies. Human recombinant IL-2 was from Glaxo. Brefeldin, anti-IFN-γ, anti-IL-17 and anti-Foxp3 from BD Biosciences.

Lentiviral Tranduction

Tfam-silenced Jurkat and Oli-Neu cells were generated by lentiviral infection. HEK293T cells were co-transfected with Lipofectamine2000 (Invitrogen) with pCMV-ΔR8.91-(Delta 8.9), pMD2.G-VSV-G and plasmids encoding shRNAs against Tfam (Open biosystems), and the corresponding control shRNAs pLKO.1 (Open Biosystems). Supernatants were collected after 48–72 h and filtered (0.45 μm). Oli-Neu cells or Jurkat T cells were subsequently transduced and selected with RPMI medium containing puromycin (4 μg ml^{-1}). Silenced cell lines were grown in the presence of 0.25 mM uridine and 1 mM sodium pyruvate.

T cell differentiation assays

Naive $CD4^+$ T lymphocytes were obtained from cell suspensions prepared from spleen and peripheral lymph nodes (LN) of *Tfam*$^{fl/fl}$ (wild type) and $CD4^+Cre^{+/wt}$ *Tfam*$^{fl/fl}$ (*Tfam*$^{-/-}$) mice. Pooled Spleen and LN cells were incubated with biotinylated antibodies to IgM, B220, CD19, CD8, Gr-1, CD44, CD25, MHC-II, F4/8, CD11c, CD11b and DX5 (BD Pharmingen) followed by streptavidin microbeads (MACS; Miltenyi Biotec). Naive $CD4^+$ T cells were obtained by negative selection using the auto-MACS Pro Separator (Miltenyi Biotec). For in vitro activation, naive $CD4^+$ T cells were incubated in RPMI 1640 (Life Technologies) supplemented with 1% sodium pyruvate, penicillin, streptomycin, 50 mM 2-mercaptoethanol and uridine (0.25 mM) and 10% FBS (Life Technologies) in the presence of 5 μg ml^{-1} plastic-bound purified anti-CD3, 2 μg ml^{-1} soluble anti-CD28 and 100 U ml^{-1} human IL-2. For Th0 conditions, anti-IFN-γ (4 μg ml^{-1}) and IL-4 (4 μg ml^{-1}) were added. For Th1 conditions, culture was supplemented with IL-12 (10 ng ml^{-1}) and anti-IL-4 (4 μg ml^{-1}). For Th2 conditions, IL-4 (10 ng ml^{-1}) and anti-IFN-γ (10 μg ml^{-1}) were added. For Th17 conditions, anti-IL-2 (10 μg ml^{-1}), anti-IL-4 (10 μg ml^{-1}), anti-IFN-γ (10 μg ml^{-1}), TGF-β (5 ng ml^{-1}), IL-23 (20 ng ml^{-1}) and IL-6 (20 ng ml^{-1}) were included in cultures. For Treg cell differentiation, TGF-β (10 ng ml^{-1}) was added.

Quantitative real-time-PCR and mtDNA analysis

Total RNA was extracted from cells using the RNeasy kit (QIAGEN) and cDNA was synthesized with the High Capacity cDNA Reverse Transcription Kit (Applied Biosystems). Triplicate reactions were run on a 7500 Fast Real Time PCR System (Applied Biosystems) using SYBR Green PCR reagents (Applied Biosystems). The expression of mRNA for genes of interest was normalized to the expression of β-actin and beta-2-microglobulin. Data were analyzed using Biogazelle QBasePlus software (Biogazelle). For analysis of mtDNA levels, total DNA was extracted with the DNeasy kit (QIAGEN). mtDNA was amplified using primers specific for the genes for mitochondrial cytochrome c oxidase subunit 1 (mtCO1) and NADH dehydrogenase 1 (mtND1) and normalized to genomic DNA by amplification of the succinate dehydrogenase (SDH) nuclear gene.

Electron microscopy

Wild-type and Tfam$^{-/-}$ lymphoblasts were fixed in 2.5% glutaraldehyde (Sigma-Aldrich) in PBS for 15 min, washed, and treated with 1% osmium tetroxide (Sigma-Aldrich) for 45 min. Samples were extensively washed with water and dehydrated through increasing concentrations of ethanol (25%, 50%, 75%, 95% and absolute). Samples were then embedded in DURCUPAN resin (Fluka) and stored overnight at room temperature. The resin column was polymerized by baking at 60°C for 48 h, and ultrathin sections were cut and contrasted. Sections were examined with a JEOL JEM1010 electron microscope (100 KV) equipped with a BioScan digital camera (Gatan). Images were monitored with DigitalMicrograph 3.1 (Gatan).

Survival assays

T lymphoblast were cultured either in RPMI 1640 containing glucose or in RPMI 1640 deprived of glucose (Life Technologies) supplemented with 5mM galactose (Sigma) and dialyzed FBS. Viable cells were analyzed by HOECHST58 exclusion by flow cytometry.

Mitochondrial content and ROS

Mitochondrial mass and mitochondrial-derived ROS levels were measured by flow cytometry after labelling cells with 50 nM Mitotracker green and 2.5 μM MitoSOX, respectively.

Extracellular flux analysis and metabolic assays

Oxygen consumption rates (OCR) and extracellular acidification rates (ECAR) were measured in a XF-96 Extracellular Flux Analyzers (Seahorse Bioscience) in cells suspended in XF medium (nonbuffered RPMI 1640 containing either 25 mM glucose or 1 mM palmitate, 2 mM L-glutamine, and 1 mM sodium pyruvate). Three measurements were obtained under basal conditions and upon addition of the mitochondrial inhibitors oligomycin (1 μM), fluoro-carbonyl cyanide phenylhydrazone (FCCP; 1.5 μM), and rotenone (100 nM) + antimycin A (1 μM).

Calcium measurement

Lysosomal calcium was measured in cells loaded with INDO-1 and fluorescence intensity ratio at 340/380 nm was detected by flow cytometry. After basal recording, cells were treated with bafilomycin-A1 (Sigma) to promote lysosomal calcium release for the indicated times.

Fluorescence confocal microscopy

For immunofluorescence assays, cells were plated onto slides coated with poly-L-lysine (50 μg ml^{-1}), incubated for 30 min, and then fixed, blocked and stained with the indicated primary antibodies (5 μg ml^{-1}) followed by alexa488- or Rhodamine Red X-labeled secondary antibodies (5 μg ml^{-1}). Samples were examined with a Leica SP5 confocal microscope (Leica) fitted with a 63X objective, and images were processed and assembled using Leica software.

Immunoblotting

Cell preparations were lysed in 50 mM Tris pH 7.5, containing 0.3 M NaCl, 0.5% Triton X-100, 0.1% NP-40, and a cocktail of protease inhibitors (Roche). Cell lysates were cleared of nuclei by centrifugation at 15,000 g for 10 min. Protein extracts were separated by 4–12% SDS–PAGE and transferred to a nitrocellulose membrane (Biorad). Proteins were visualized with LAS-3000 after membrane incubation with specific antibodies (5 μg ml^{-1}) and secondary antibodies conjugated to peroxidase (5 μg ml^{-1}). Band intensities were quantified using ImageJ software (NIH) and results are expressed relative to controls. Cell fractionation assays were performed using ProteoExtract Subcellular Proteome Extraction Kit (Calbiochem).

Lipidomic analyses

Ultra performance liquid chromatography coupled to mass spectrometry (UPLC-MS) was used for optimal profiling of glycerolipids, glycerophospholipids, sterol lipids and sphingolipids as described in (Barr et al., 2012). Briefly, cells were lysed and proteins precipitated by adding 4 volumes of methanol at room temperature. After brief vortex mixing, chloroform was added to the samples at room temperature. Samples were incubated at -20 °C for 30 min and after brief

vortex cell extracts were mixed with water (pH=9). Following brief vortex mixing, the samples were incubated for 1 hr at -20 °C and afterwards centrifuged at 16,000 x g for 15 min. The organic phase was collected and dried by speed-vacuum centrifugation. Dried extracts were then reconstituted in acetronitrile/isopropanol (1:1), centrifuged (16,000 x g for 5 min), and transferred to vials for UPLC-MS analysis. Data pre-processing generated a list of chromatographic peak areas for the metabolites detected in each sample injection. Data were normalized using the procedure described in (van der Kloet et al., 2009). Univariate statistical analyses were performed to calculate group percentage changes, and unpaired Student's t-test (or Welch's t test where unequal variances were found) was used to compare $Tfam^{-/-}$ and wild-type T lymphocytes.

Induction of a contact hypersensitivity (CHS) response

CHS was induced by painting shaved mouse abdomen skin with 200 µl 3% oxazolone (4-Ethoxymethylene-2-phenyl-2-oxazolin-5-one, Sigma) in ethanol. After 4 days mice were challenged with 20 µl 1% oxazolone on each side of the right ear. The left ear was painted with vehicle as a control. Ear thickness was measured every day for nine days. For analysis of the in vivo Th1 response, ear lymph nodes were removed from mice 5 days after challenge, single-cell suspensions were prepared, and intracellular staining of activated $CD4^+$ T cells for IFN-γ was performed as described above.

Blue-native gel electrophoresis, mitochondrial complex activities, and mitochondrial membrane potential assays

Cellular lysates from wild-type and *Tfam*$^{-/-}$ T lymphocytes were lysed in the presence of digitonin and proteins separated on 5–13% gradient blue-native gels (Lapuente-Brun et al., 2013). Total ATP and mitochondrial derived-ATP synthesis in T cell lysates was measured by a kinetic luminescence assay. The activities of individual complexes were measured spectrophotometrically as previously described (Acin-Perez et al., 2014). For mitochondrial potential assays, resting and activated cells were labelled with tetramethylrhodamine methyl ester

(TMRM, 100 nM), and analyzed by flow cytometry upon incubation with oligomycin (200 nM) for the indicated times.

Flow cytometry analysis

Viable cells were identified by HOECHST58 exclusion. Singlet cells were discerned with a stringent multiparametric gating strategy based on FSC and SSC (pulse width and height). For surface labeling, cells were stained with antibodies diluted in PBS-0.5% BSA on ice. Cell suspensions from thymus, spleen and lymph nodes were blocked with Fc-block (CD16/CD32, BD Biosciences), washed in PBS and 1% BSA and incubated with the following primary antibodies diluted in PBS and 1% BSA: CD11b, CD11c, B220, CD3, CD4, CD8 and CD45.1 (BD Biosciences). For intracellular and surface staining, cells fixed with 1% formaldehyde were stained with the indicated primary and secondary antibodies diluted in PBS-0.5% BSA and 0.5% Saponin. Cell sample data were acquired on a FACSCanto flow cytometer and analysed using FACSDiva software (BD Biosciences) and FlowJo software.

ELISA

$CD4^+$ T cells activated with CD3/CD28 or in the different polarization conditions (6 days) were washed and cultured in equal numbers in fresh medium followed by restimulation with PMA/ionomycin (16 hr). Cell culture supernatants were assayed for mouse IL-6, IL-4, IL-17, IL-10 and IFN-γ (from eBioscience) by enzyme-linked immunosorbent assay (ELISA) based on colorimetric quantification. The absorbance at A405 nm was measured in a microplate reader (Bio-Rad Model 550) and results were expressed as means of duplicate wells.

DSS-induced colitis model

Colitis was induced in wild-type and *Tfam*$^{-/-}$ mice by daily administration of 3% Dextran Sodium Sulfate (DSS, Mw 30.000–40.000) for 7 days in drinking water. The clinical parameters used to score the disease were weight loss, loose stools/diarrhea and presence of occult/gross bleeding (Cooper et al., 1993). The animals were weighed before starting the treatment (initial weight) and every day until the end of the treatment. Animals were also checked daily for stool consistency

and for the presence of blood in the stools. At the end of treatment, colons were processed for histological analysis to check for the presence of infiltrates in the lamina propia, and mesenteric lymph nodes were processed to study cytokine production of immune cells by flow cytometry.

Lysosomal content, pH and activities

Analysis of Cathepsin B activity was performed in wild-type and *Tfam*$^{-/-}$ T-lymphoblasts with the Magic Red™ Cathepsin B detection kit (Immunochemistry Technologies). Cells were incubated 30 min with Magic Red™ and the fluorescence intensity was measured by flow cytometry. Acid phosphatase activity (Sigma) and acid sphingomyelinase activity (AAT Bioquest) were performed in total cell lysates from T-lymphoblasts following manufacturer's instructions. Lysosomal pH was determined with the ratiometric lysosomal pH probe LysoSensor™ Yellow/Blue DND-160 (Life Technologies). LysoSensor DND-160 undergoes a pH-dependent emission shift to longer wavelengths in acidic environments. Briefly, T-lymphoblasts were labelled with 2 μM LysoSensor™ Yellow/Blue DND-160 for 30 min at 37 ºC. Lysosomal pH was detected by dual-excitation and dual-emission measurements by flow cytometry. Lysosomal content was determined by flow cytometry after incubation with Lysotracker.

Confocal microscopy analysis of autophagy and mitophagy

LC3-GFP-RFP tandem construct was a gift from Tamotsu Yoshimori (Addgene plasmid # 21074). pEGFP-parkin WT was a gift from Edward Fon (Addgene plasmid # 45875). For autophagosome-lysosome fusion assays, shControl and shTfam Oli-Neu cells were transfected using Lipofectamine (Invitrogen) with LC3-GFP-RFP, and left untreated or treated with Rapamycin (Sigma) during 3 hr and LC3-GFP/RFP fluorescence was examined with a Leica SP5 confocal microscope (Leica) fitted with a 63X objective. Cells were acquired with the same laser parameters using the same image magnification. Images were processed and assembled using Leica software. The number of GFP, RFP and GFP- RFP-positive autophagosomes were analyzed using Image J imaging software (NIH). For mitophagy assays, shControl and shTfam Oli-Neu cells transfected with Parkin-GFP were left untreated or treated with carbonyl cyanide m-

chlorophenyl hydrazone (CCCP, Sigma) during 3 hr and Parkin-GFP fluorescence was examined with a Leica SP5 confocal microscope (Leica) fitted with a 63X objective. Images were processed and assembled using Leica software and the area of Parkin-GFP fluorescence was analyzed with Image J imaging software (NIH).

Supplemental References

Acin-Perez, R., Carrascoso, I., Baixauli, F., Roche-Molina, M., Latorre-Pellicer, A., Fernandez-Silva, P., Mittelbrunn, M., Sanchez-Madrid, F., Perez-Martos, A., Lowell, C.A., et al. (2014). ROS-Triggered Phosphorylation of Complex II by Fgr Kinase Regulates Cellular Adaptation to Fuel Use. Cell Metab 19, 1020–1033.

Barr, J., Caballeria, J., Martinez-Arranz, I., Dominguez-Diez, A., Alonso, C., Muntane, J., Perez-Cormenzana, M., Garcia-Monzon, C., Mayo, R., Martin-Duce, A., et al. (2012). Obesity-dependent metabolic signatures associated with nonalcoholic fatty liver disease progression. J Proteome Res 11, 2521-2532.

Cooper, H.S., Murthy, S.N., Shah, R.S., and Sedergran, D.J. (1993). Clinicopathologic study of dextran sulfate sodium experimental murine colitis. Lab Invest 69, 238-249.

Lapuente-Brun, E., Moreno-Loshuertos, R., Acin-Perez, R., Latorre-Pellicer, A., Colas, C., Balsa, E., Perales-Clemente, E., Quiros, P.M., Calvo, E., Rodriguez-Hernandez, M.A., et al. (2013). Supercomplex assembly determines electron flux in the mitochondrial electron transport chain. Science 340, 1567-1570.

van der Kloet, F.M., Bobeldijk, I., Verheij, E.R., and Jellema, R.H. (2009). Analytical error reduction using single point calibration for accurate and precise metabolomic phenotyping. J Proteome Res 8, 5132-5141.